ISAS - INTERNATIONAL SCHOOL
FOR ADVANCED STUDIES

Sodium Currents on Rat Cerebellar Granule Cells

Thesis submitted for the degree of
"Magister Philosophiae"

CANDIDATE
Fan Lin

SUPERVISORS
Prof. Antonio Borsellino
Dr. Zygmunt Galdzicki
Dr. Oscar Moran

October 1988

TRIESTE

SISSA - SCUOLA
INTERNAZIONALE
SUPERIORE
DI STUDI AVANZATI
TRIESTE
Strada Costiera 11

International School for Advanced Studies
Trieste

Sodium Currents on Rat cerebellar Granule cells

Thesis submitted for the degree of
"Magister Philosophiae"

CANDIDATE
Fan Lin

SUPERVISORS
Prof. Antonio Borsellino
Dr. Zygmunt Galdzicki
Dr. Oscar Moran

October 1988

Contents

Introduction 1

1 Review of Hodgkin-Huxley model 3
- 1.1 Membrane potential 3
- 1.2 Action potential 5
- 1.3 Voltage clamp technique 8
- 1.4 Hodgkin-Huxley model 8

2 Material and Method 16
- 2.1 Cell culture 16
- 2.2 Solutions 17
- 2.3 Preparation of patch pipette 21
- 2.4 Whole cell patch clamp equipment 21
- 2.5 Experimental design 25

3 Results 28
- 3.1 The action potential and whole cell sodium current . . . 28
- 3.2 Activation process of sodium channel 30
  - 3.2.1 Steady state activation probability 30
  - 3.2.2 Time constant of activation process 34
- 3.3 Inactivation process of sodium channel 36
  - 3.3.1 Steady state inactivation probability 36
  - 3.3.2 Time constant of inactivation process 36

4 Discussion 40
- 4.1 Discussion 40

4.1.1 Properties of sodium channel in rat granule cell . 41
4.1.2 Comparision of the earlier and later experiments 41
4.1.3 Series resistance compensation 44
4.2 Conclusions 46

Bibliography **47**

Acknowledgements **52**

Introduction

Granule cells are the main component of the granular layer of the mammalian cerebellar cortex, coordination center of the body movements. They are extremely small neurons with a high packing density matched almost nowhere else in the brain. The granule cells can accept the electrical messages from the axons of peripheral nervous system and transfer the messages through their own axons to the neurons in more superficial parts of the cortex. Therefore, the granule cells are highly excitable and can be used to study the permeability changes of the channels during the action potential.

In the quantitative studies of ionic permeability changes of excitable cell membranes during excitation, the Hodgkin-Huxley (HH) model has been proved to be the most efficient and practical one [1]. Based on experimentally measurable parameters, the HH model provides a physical interpretation of the excitability in cells.

In this thesis, we analyze the properties of the whole cell Na currents in primary cultured rat cerebellum granule cells, using the patch-clamp technique [2]. Our study shows that cells after 24 hours in culture can be used to study the properties of sodium channels [3]. We have used two approaches to obtain the pure Na currents: blocking the K currents with CsF; or subtracting the K currents obtained by blocking Na channels with TTX (Tetrodotoxin, from puffer fish) from the total currents. Our experiments show that the subtracting method is not reliable, it drops much time and hence introducing instability of the patch condition.

The sodium current was analyzed according to the HH model. The classic two-pulse experiment has been done to obtain the inactivation

parameter (h_∞). Other parameters of the model, namely m_∞, τ_m and τ_h were obtained by fitting Na currents obtained in our one-pulse experiments.

The results were in good agreement with the predictions of the HH model and comparable with results obtained in the other excitable cells [4,5,6,7]. We have also studied the temperature dependence of the time constants. The temperature-dependent activation process has been observed. Sodium channel parameters in the granule cells have been found to be comparable to those in other neurons.

The thesis is organized in the following way: For completeness, we give a description of the HH model in chapter 1; in chapter 2 the material preparations and experimental designs are presented; in chapter 3, the data analysis and results are detailed; finally, we compare our results with those obtained by others together with discussions in chapter 4.

Chapter 1

Review of Hodgkin-Huxley model

Many species of cells such as neurons and muscle cells are able to produce and transduce electrical signals as a response to outside stimulations. The cells with this ability are called excitable cells, and this ability is called excitability. The response (electrical signal) is called action potential.

1.1 Membrane potential

Each living cell is limited by a low-conductance membrane which separates the ion-rich high conductance intracellular from the extracellular compartments [8]. The hydrophobic nature of the lipid bilayer of the cell membrane gives rise to different mechanisms for the ionic permeability through the membrane. The ionic channels, ionic carriers and the energy-driven pumps are among the most important mechanisms for the electric transport through the membrane, each of which has different permeability for different ionic species. Figure 1.1 shows a working hypothesis of the ionic channel [1].

The ionic channel is a transmembrane protein sitting in the lipid bilayer of the membrane. When open, the channel forms a water-filled pore extending fully across the membrane, so that the ions can pass.

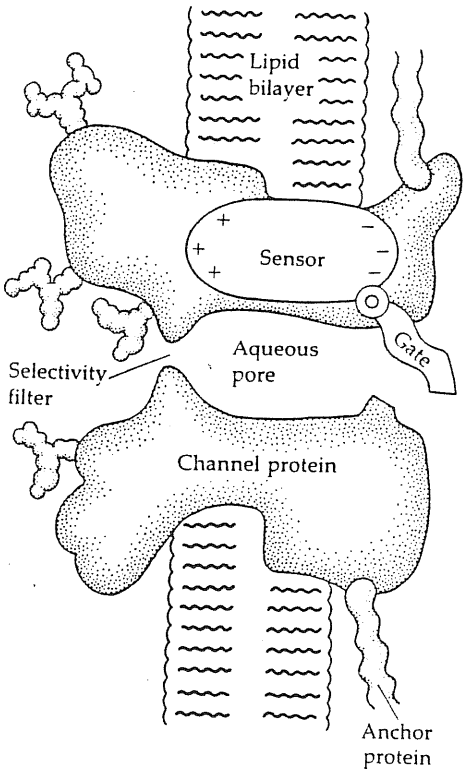

Figure 1.1:

Working hypothesis for a channel.

The channel is drawn as a transmembrane macromolecule with a pore through the center. The functional regions, selectivity filter, gate, and sensor are deduced from voltage-clamp experiments but have not yet been charted by a structure study [1].

Different kinds of ionic channels have different pore sizes, which lead to the ionic selectivity of the channel, and different gate charges, which result in different voltage dependence. The different ionic channels, the carriers and the pumps make the ionic concentrations and ionic types on both sides of the membrane different. It is these differences in ionic concentrations and types on the two sides which generate the electrical potential difference across the membrane. This potential is called membrane potential, and is defined as inside membrane potential minus the outside one (the outside membrane potential is grounded) [1].

Assuming that the membrane is only permeable to one kind of ions, the ions will transfer from one side of the membrane to the other, until an equilibrium potential across the membrane is established. This potential can be calculated by the Nernst equation [9]:

$$V_n = \frac{RT}{z_s F} \ln \frac{[n]_o}{[n]_i} \tag{1.1}$$

where R is the ideal gas constant, T the absolute temperature , z_s the electrical valence of the ion and F the Farady's constant. The two quantities $[n]_o$ and $[n]_i$ are the extracellular and intracellular concentrations of the ion respectively. The Ohm's law, when applied to describe the currents through the ionic channels, should be:

$$I_n = g_n(V - V_n), \tag{1.2}$$

where g_n is the conductance of the channel, and V_n is the equilibrium potential which is also called "electromotive force" (EMF) of the channel.

1.2 Action potential

The action potential is generated by the depolarization of the membrane caused by the flow of ions through the ionic channels, in response to the external stimulation. It sharply rises and propagates along the cell membrane.

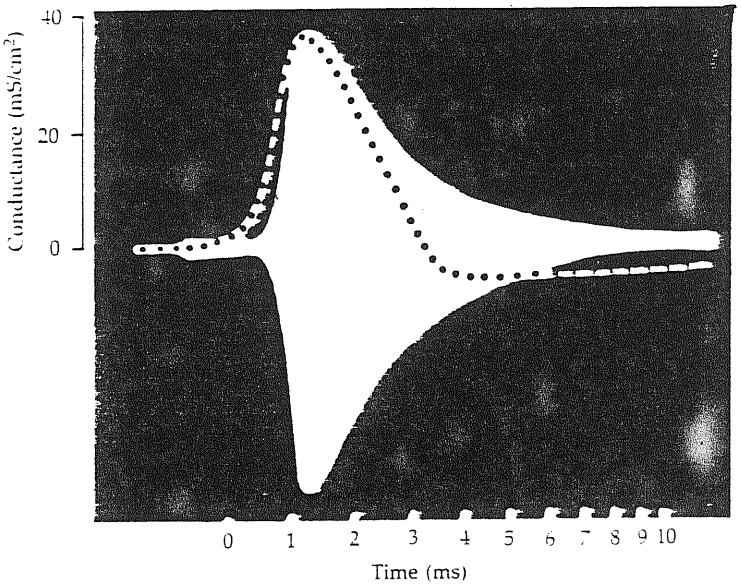

Figure 1.2:

The conductance increase in excitation.

This classical picture is the first direct demonstration of an ionic permeability increase during the propagated action potential. The time course of membrane conductance increase in a squid giant axon is measured by the width of the white band photographed from the face of an oscilloscope during the action potential (Dotted line) [10].

Figure 1.2 shows the first demonstration of ionic permeability increase during activity, obtained by Cole and Curtis [10]. They used a Wheststone bridge to study the membrane impedance changes of the squid giant axon during the propagated action potential. They found that:

- Each action potential is accompanied by a dramatic impedance decrease (i.e. 40-fold conductance increase);
- Membrane conductance is a function of voltage and time. It increases only after the membrane potential has risen several millivolts from the resting potential;
- EMF of membrane changes during the action potential, which implies that there are more than one kind of ions takeing part in the activity.

A more detailed study on the squid giant axon excitability was carried out by Hodgkin and Katz [11]. They designed some experiments to study the amplitude change of the action potential by replacing a fraction of NaCl in the extracellular solutions with choline chloride, glucose or sucrose. Based on the experimental results, they proposed a "sodium theory" in which they concluded that the resting membrane is mainly permeable to the potassium ions and the action potential is mainly due to the inward-rushing of sodium ions.

Although the studies of action potential had qualitatively established important concepts of the ionic hypothesis of the action potential, it was found that they could not provide any quantitative bases because the time variations of the current, conductance and voltage make the Ohm's law (equation 1.2) insoluble. In order to solve this problem, a new experimental procedure called "voltage clamp" was developed by Marmont and Cole [12,13], and was used by Hodgkin, Huxley and Katz in a series of formidable experiments [14,15].

1.3 Voltage clamp technique

"Voltage clamp" is a technique, by which the experimenter controlls voltages across the membrane and measures the current. Most voltage clamp devices are composed of two intracellular electrodes. One electrode is used to measure the membrane potential, and a negative feedback amplifier is connected with it to amplify any difference between the recorded voltage, and the value of the membrane potential desired. The other intracellular electrode is used for injecting current from the output of the amplifier, to eliminate the difference between the measured and the desired membrane potentials. With this arrangement, the membrane potential is kept constant and the current is measured. Figure 1.3 shows simplified arrangements for the voltage clamping of the cell membrane.

The total current measured can be expressed as:

$$I = C_m \frac{dV}{dt} + I_i \tag{1.3}$$

where I is the total currents across the membrane, and I_i is the ionic currents through the channels. $C_m \frac{dV}{dt}$ is the "capacity-component" of the current (hereinunder, we call it capacity current) due to the depolarization of the cell membrane. Since the derivative $\frac{dV}{dt}$ is the variation of membrane potential with time, the capacity current is not zero only at the onset and offset of the voltage (the voltage is constant during the clamping). The capacity current varies almost linearly with the voltage, and therefore can be subtracted easily. So the voltage clamp provides a direct way to measure the total ionic flow through the channels.

1.4 Hodgkin-Huxley model

With the voltage clamp technique, Hodgkin and Huxley [7,16,17,18] designed a series of experiments with squid giant axons. They confirmed quantitatively their "sodium theory" and modelled the axon membrane by an electrical circuit with four parallel branches, each representing the membrane capacitance and sodium, potassium and "leakage" channel

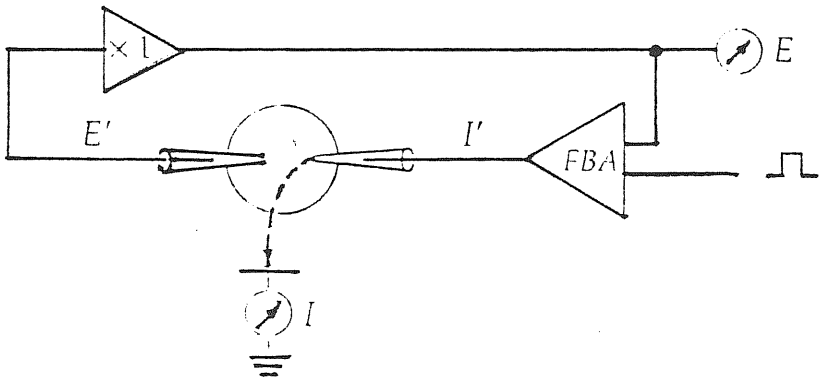

Figure 1.3:

Design of voltage-clamp method.

E' is a voltage recording electrode, I' is a current-delivering electrode. The voltage electrode connects to a high impedance follower circuit. The output of the follower is recorded at E and compared with the voltage-clamp command pulses by a feedback amplifier (FBA). The highly amplified difference of these signals is applied as a current (dash arrows) through I', across the membrane, and to the bath-grounding electrode, where it can be recorded (I) [1].

conductances, as well as the electromotive forces of the channels (see figure 1.4).

They found that the channel conductance increases follow a S-shaped time course, when the membrane starts to be depolarized, and decreases exponentially as the membrane is repolarized. They also revealed that during the membrane depolarization, the sodium channel conductance changes due to two processes, namely *activation* and *inactivation.* The activation is a rapid process that opens Na channels during the depolarization, while the inactivation is a slow process that closes Na channels during a depolarization. The potassium conductance is always slowly activated during the depolarization, but not inactivated. Figure 1.5 shows clearly the difference between the two conductances.

Based on these features, Hodgkin and Huxley conjectured that there were four charged particles, called *gate particles*, for controlling the potassium and sodium channels. According to the HH model, there are only two configurations of the gating particles: *permissive* and *non-permissive.* If the gate particles are in the permissive positions, the channel is opened, otherwise the channel is closed.

Let us define a probability variable n, which assumes value $n = 1$ if a gating particle is in its permissive configuration, and $n = 0$ when it is in its non-permissive configuration. Using this description, the current through the potassium channel can be expressed as:

$$I_k = n^4 \bar{g}_k (V - V_k) \tag{1.4}$$

where $\bar{g}_k$ is the maximum value of K conductance. Assuming a first order kinetics of the change between open and closed states, the variation of n can be expressed with the equation:

$$\frac{dn}{dt} = \alpha_n (1 - n) - \beta_n n \tag{1.5}$$

with α_n and β_n being two voltage-dependent rate constants of gating particle transition between its permissive and non permissive positions. The solution of equation 1.5 is easily obtained:

$$n(t) = n_\infty - (n_\infty - n_0) \exp(-\frac{t}{\tau_n})$$

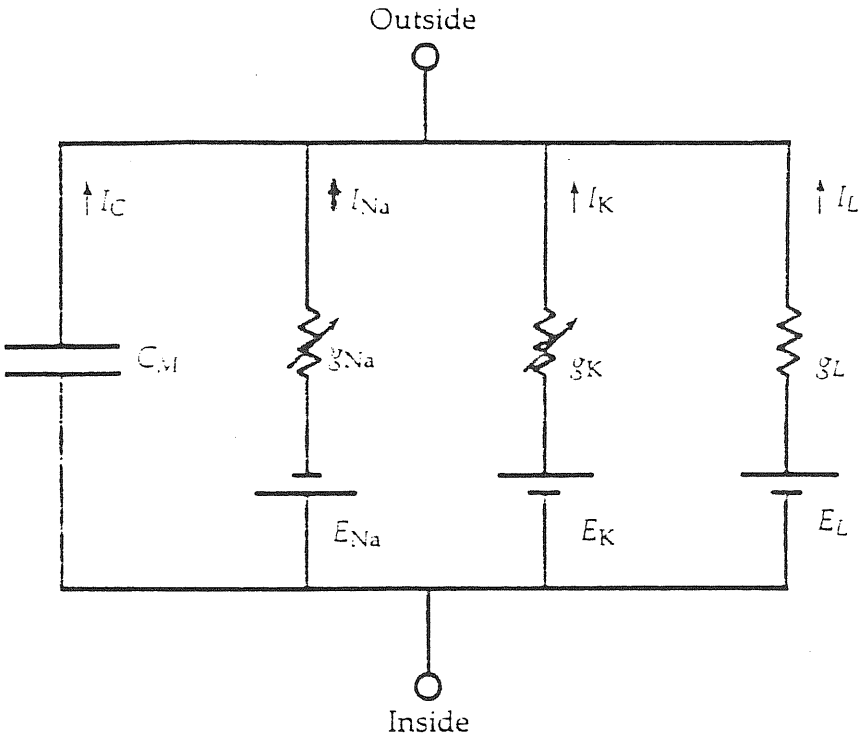

Figure 1.4:

Equivalent circuit of axon membrane.

Hodgkin and Huxley described the axon membrane as an electrical circuit with four parallel branches. The capacity branch represents the dielectric properties of the membrane. The three conductive branches represent sodium, potassium and leak conductance with their different electromotive forces. The vertical arrows define the direction of positive current, according to new convention. The variable resistors denote time- and voltage-varying conductance arising from the opening and closing of ionic channels [7].

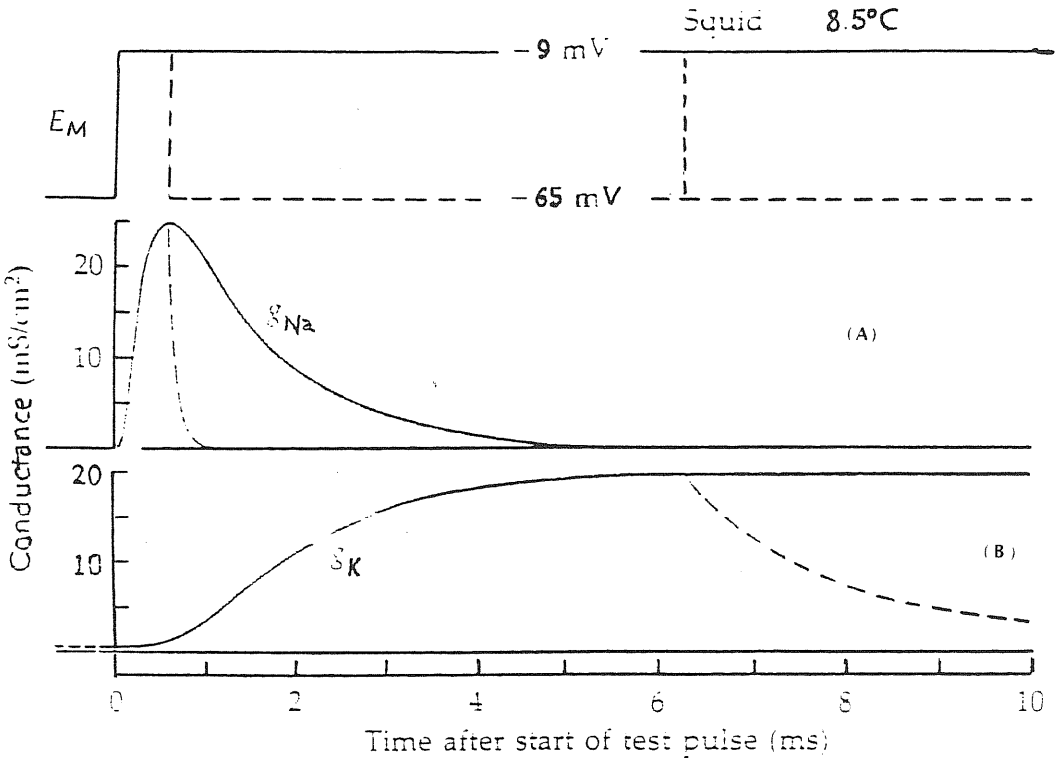

Figure 1.5:

Ionic conductance changes in squid axon.

(A) show the two processes of sodium conductance change, and the one of potassium conductance change (B) during the depolarization. The dash line shows the exponential decreases of Na and K conductances [19].

$$\begin{aligned} \tau_n &= \frac{1}{\alpha_n + \beta_n} \\ n_\infty &= \frac{\alpha_n}{\alpha_n + \beta_n} \end{aligned} \tag{1.6}$$

where τ_n is the time constant of activation process, and n_∞ is the steady state activation probability, n_0 is the activation probability at $t = 0$.

Figure 1.6 shows the potential dependence of τ_n and n_∞ obtained by fitting the potassium current with equation 1.6. It can be seen that at very low potential (e.g. $-75mV$), n_∞ is small, which implies that potassium channels tend to close. At positive potential (e.g. $+50mV$), n_∞ is close to one, which implies the channels tend to open. τ_n is large at low potential, and small at high potential, i.e the activation process is slow at low potential, and faster with the increase of potential.

The description for sodium current is quite similar to that for potassium current. As the sodium current depends on two different processes during the depolarization, it has been assumed that the four gating particles can be divided into two types for controlling the opposite processes. The activation process is controlled by three gating particles at permissive configuration, while inactivation process is controlled by the configuration of the last particle. The sodium current can be described by the following equation:

$$I_{Na} = m^3 h \bar{g}_{Na}(V - V_{Na}) \tag{1.7}$$

where the activation probability m follows the the first order kinetics equation:

$$\frac{dm}{dt} = \alpha_m(1 - m) - \beta_m m \tag{1.8}$$

and the first order kinetics of the not inactivation probability h is described by:

$$\frac{dh}{dt} = \alpha_h(1 - h) - \beta_h h \tag{1.9}$$

where the parameters α and β (we ommitted the subscripts) are the voltage dependent rate constants of transient processes between permissive positions and non-permissive positions. The solutions of the

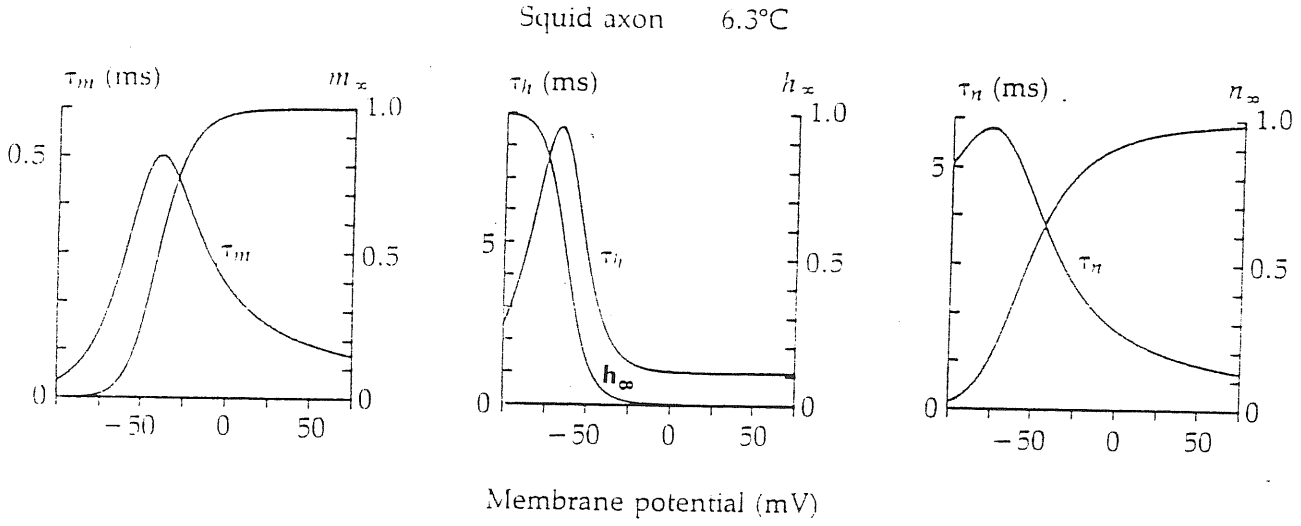

Figure 1.6:

Voltage-dependent parameters of HH model.

Time constants τ_m, τ_h, τ_n and steady state values m_∞, h_∞ and n_∞ ,as obtained from the empirical equations of the HH model for squid giant axon membrane at $6.3°C$. Depolarizations increase m_∞ and n_∞ and decrease h_∞ [20].

equations 1.8, 1.9 are given by:

$$\begin{aligned} m(t) &= m_\infty - (m_\infty - m_0)\exp(-\frac{t}{\tau_m}) \\ \tau_m &= \frac{1}{\alpha_m + \beta_m} \\ m_\infty &= \frac{\alpha_m}{\alpha_m + \beta_m} \end{aligned} \tag{1.10}$$

and

$$\begin{aligned} h(t) &= h_\infty - (h_\infty - h_0)\exp(-\frac{t}{\tau_h}) \\ \tau_h &= \frac{1}{\alpha_h + \beta_h} \\ h_\infty &= \frac{\alpha_h}{\alpha_h + \beta_h} \end{aligned} \tag{1.11}$$

Here the parameters for the activation process have the similar implications to those for potassium channel. And h is the probability of not-inactivation in steady state of sodium channel, τ_h is the time constant of the inactivation process. Figure 1.6 (a) and (b) show the potential dependence of m_∞, τ_m, h_∞ and τ_h. We see that the activation process is much faster than the inactivation process and the steady state parameters m_∞ and h_∞ behave in opposite ways.

The purpose of the HH model was to explain the classical phenomena of electrical excitability through quantitative analysis of voltage-clamp current. The model has demonstrated the importance of Na and K permeability changes for excitability, as well as described the kinetics of the permeability changes quantitatively. However, the most important feature of the model is that it provides the physical interpretation to the excitability and provides a series of measurable parameters to characterize the ionic channels. For these reasons, this model has been demonstrated to be a useful tool in the studies of voltage-dependent ionic currents in most of the excitable cells for more than 35 years.

Chapter 2

Material and Method

We have carried out a series of experiments to study the permeability changes of sodium channels during the excitation of the primary cultured rat cerebellar granule cells. Since this cell has a diameter of about 5 to 10 μm, the classic intracellular electrodes voltage-clamp technique cannot be used. In our experiments, we used the whole cell patch-clamp technique, which is still one of the voltage-clamp configurations [2].

2.1 Cell culture

The primary cultures of rat cerebellar granule cells were prepared from 8-day-old postnatal pups with the following procedure [21]. Groups of 8 rat cerebella were washed with *Krebs solution* (see tab. 2.1) and were sliced with a sterile razor in two orthogonal directions. The sliced cerebella were suspended and centrifuged at low speed for 1 minute in solution 1 described in table 2.2. The pellet was resuspended by solution 2 (see table 2.3) for 12 $\sim$ 15 minutes in which the Trypsin digested the connective tissues between the cells. The trypsinization process was stopped by Soybean Trypsin Inhibitor in solution 3 (see table 2.4). The cells were washed 2 $\sim$ 3 times in solution 4 (see table 2.5), obtaining a quite purified granule cell pellet. The pellet was suspended in neuron growth medium (see table 2.6) and plated at a density of 1×10^6 cell/dish in poly-L-Lysine coated $35mm$ Falcon dishes. $10\mu M$ Cytosine

Compositions	*Concentrations* (mM)
NaCl	124.00
KCl	5.37
$NaH_2PO_4 \cdot H_2O$	1.01
$D-glucose$	14.50
phenol red	0.027
HEPES	25.00

Table 2.1:

Krebs solution

pH of the solution is adjusted to 7.4 using NaOH.

arabinoside was added to all dishes after 19 hrs. *in vitro* culture to inhibit the replication of non-neuronal cells. The cultures were maintained at $37°C$ at a 100% humid atmosphere with $5\%CO_2 - 95\%$ air up to even one month. Under this condition, 90% granule cells per dish were obtained [21]. All cells used were after 24 hours *in vitro* culture so that the cells were strongly attached to the bottom of the dishes.

2.2 Solutions

Two sets of intra/extra-cellular solutions were used during the recording. Table 2.7 describs the first set of solutions, in which there was no blocker for the potassium channels. In this case, TTX $(1\mu M)$ was added to the extracellular solution bath to block the Na channels after the control recordings were made. Table 2.8 gives the second set of solutions which were used in later recordings. CsF in the intracellular solution directly blocks the potassium currents. There was no difference in the current record with or without Ca channel blockers (see [3]). It suggests that Ca channels do not exist in rat granule cells.

Compositions	*quantities*
Krebs solution	15 ml
distilled H_2O	135 ml
Bovine serum Albumin	0.45 g
$MgSO_4 \cdot 7H_2O$	22.4 mM

Table 2.2:

Solution 1

pH of the solution is adjusted to 7.4 using NaOH.

Compositions	*Quantities*
Solution 1	50 ml
trypsin	12.5 mg

Table 2.3:

Solution 2

Compositions	*quantities*
solution 1	15 ml
DNase	1.2 mg
Soybean trypsin inhibitor	7.8 mg
$MgSO_4 \cdot H_2O$	2.8 mM

Table 2.4:

Solution 3

Compositions	*quantities*
solution 1	12.5 ml
$CaCl_2 \cdot H_2O$	1.2 mM
$MgSO_4 \cdot H_2O$	1.6 mM

Table 2.5:

Solution 4

Compositions	*quantities*
Basal Medium Eagle	500.0 ml
L-glutamine	147.0 mg
KCl	825.0 mg
gentamicin	50.0 mg
fetal calf serum	
(heat inactivated)	50.0 ml

Table 2.6:

Neuron growth medium

Intracellular		*Extracellular*	
KCl	125.00 mM	$NaCl$	150.0 mM
$MgCl_2$	2.00 mM	KCl	3.0 mM
$CaCl_2$	0.1 mM	$CaCl_2$	1.5 mM
EGTA	1.1 mM	$MgCl_2$	1.0 mM
HEPES / KOH	5.0 mM	HEPES/$NaOH$	10.0 mM
sucrose	10.0 mM	D-glucose	6.0 mM
pH	7.2	pH	7.4

Table 2.7:

The first set of intracellular / extracellular solutions

This set of solutions is for the TTX experiment (see text).

Intracellular		*Extracellular*	
$NaCl$	10.0 mM	$NaCl$	160.0 mM
CsF	110.00 mM	$CaCl_2 \cdot 2H_2O$	2.0 mM
EGTA	11.00 mM	$MgCl_2 \cdot 6H_2O$	1.0 mM
HEPES	10.00 mM	HEPES	10.0 mM
pH	7.4	pH	7.4

Table 2.8:

The second set of intracellular / extracellular solutions

This set of solutions is for the direct Na measurement.

2.3 Preparation of patch pipette

Borosilicate-glass capillaries (*Bo-Kapillaries, Hilgenberg, FRG*) with leng th of $100mm$, inner diameter $1.05mm$ and outer diameter $1.5mm$ were used to make the patch pipettes.

Patch pipettes were pulled by a horizontal microelectrode puller (*BB-CH, MECANEX SA, Geneva, Switzerland*) at mode 4. The patch pipette obtained had an inside tip diameter about $0.7\mu m$ and had the resistances range from 3 to 10 $M\Omega$ when filled with the experimental intracellular solutions, and with extracellular solutions in the bath.

2.4 Whole cell patch clamp equipment

The whole cell current recording manipulation and equipment arrangements were made according to the procedure described by Hamill and his collaborators in 1981 [2].

The patch-clamp equipment is essential made of two separate parts. The first is an I-V converter, which is mounted on the micromanipulators and directly connected with the pipette holder (shown in figure 2.1). The pipette current is obtained from the voltage drop across the high-value resistor R_f inside the converter. The second part is the patch amplifier (shown in figure 2.2). It contains several functional elements:

- the potential differential amplifier (A_2 in figure 2.2), for monitoring the difference between the command voltage and the measured voltage;
- the transient-cancellation amplifier (A_5), for cancelling pipette capacitance (C_{fast}), and compensating the membrane capacitance (C_{slow}). After such compensation, the membrane capacitance value can be read directly from the dial setting of the amplifier;
- the series resistance compensation amplifier (A_3), for compensating the large series resistance created between the output of the amplifier and the cell membrane.

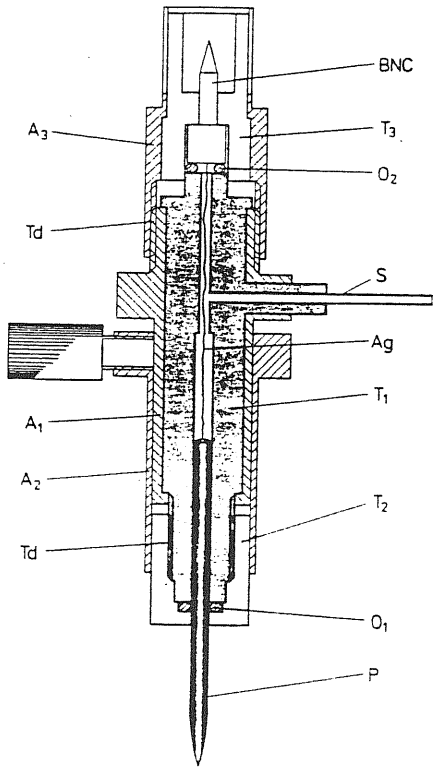

Figure 2.1:

Cross section through suction pipette holder.

The holder serves two basic functions, first to provide electrical connection between the patch pipette solution and the pin of a BNC connecter (through electrode $Ag/AgCl$), second to allow suction or pressure to be applied to the pipette interior (S) [2].

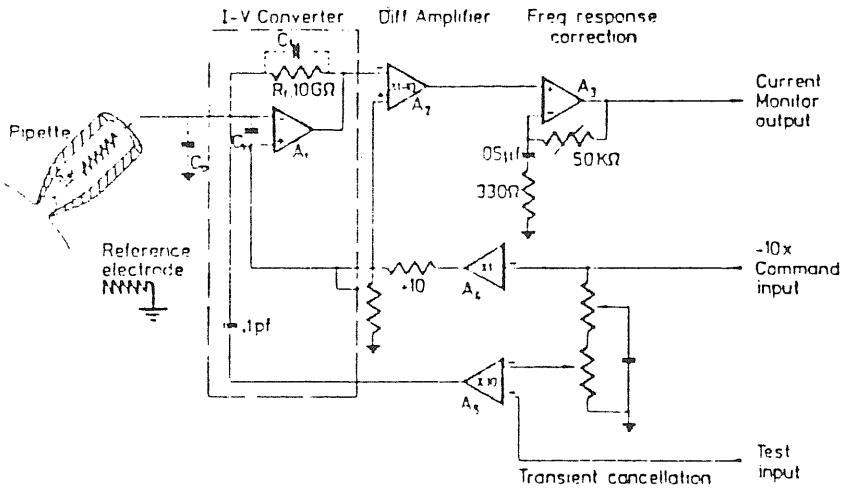

Figure 2.2:

Simplified diagram of recording system.

The current-voltage converter is mounted on a micromanipulator. The pipette holder plugs directly into the converter [2]. In our amplifer, $R_f = 500M\Omega$ for thw whole cell recording and $R_f = 50G\Omega$ for the single channel recording.

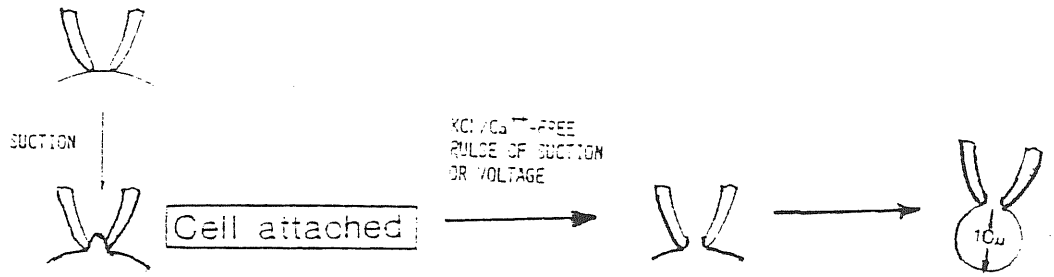

Figure 2.3:
The schematic representation of procedure of the whole cell patch-clamp recording.
The left sketch is the configuration of a pipette in a simple mechanical contact with the cell. Voltage clamp currents from whole cells can be recorded after disruption of the patch membrane (center sketch) if cells of sufficiently small diameter (right sketch) are used [2].

Figure 2.3 illustrates schematically the procedure of the whole cell recording. All the procedures were done under the microscope (*IM35 Carl Zeiss, Oberkochen, FRG*). A micromanipulator (*step motor, Zeiss, Oberkochen. FRG*) was used to approach the pipette to the cell sur-

face. The control potential application and current measurement were obtained by using a patch amplifier (*EPC-7 list, Darmstadt FRG*). Current signals were observed on oscilloscope (*TEKTRONIX 511A Beaverton USA*). In some experiments (the earlier experiments, see chapter 4.1, section 4.1.2), the stimulation voltage steps were generated with a pulse generator (*pu 8085 model, Geneva, Switzerland*). The currents were filtered through a Butterworth filter (*3202 model KROHN-HITE*) at a cut-off frequence of $3kHz$. The data of this part of the experiments were digitized and stored by the **DATAC** (*Geneva, Switzerland*) acquisition system in combination with an IBM PC-AT microcomputer. In order to simplify the data analysis and make the operation more automatic, the whole stimulation system was improved in the later experiments (see chapter 3) using a new system. The new acquisition system used a 12-bit digital-to-analog conversion board (*RT1-815, Analog Devices, USA*), combining with an Olivetti M24 microcomputer, driven by a program written in Quick Basic(*Microsoft,USA*). This program generates the stimulation voltage pulse patterns completely in a automatic way according to the pre-defined protocols.

2.5 Experimental design

In order to study the permeability of the sodium channel in the granule cell during the electric excitation, we have measured the four parameters of the HH model (see chapter 1). As external electrical stimulation, we have used two kinds of potential pulse protocols.

The first set was one-pulse experiments, by which we obtained the steady state activation parameter m_∞, as well as the time constants of activation and inactivation processes. In this one-pulse experiment, the depolarization steps, as shown in figure 2.4, were chosen to vary from $-100mV$ to $40mV$ with a duration $10msec$ in the earlier experiments (see chapter 4.1,section 4.1.2), and from $-50mV$ to $60mV$ in later improved experiments, with duration of $7msec$. In the earlier experiments, the linear leakage and capacity currents were eliminated through the

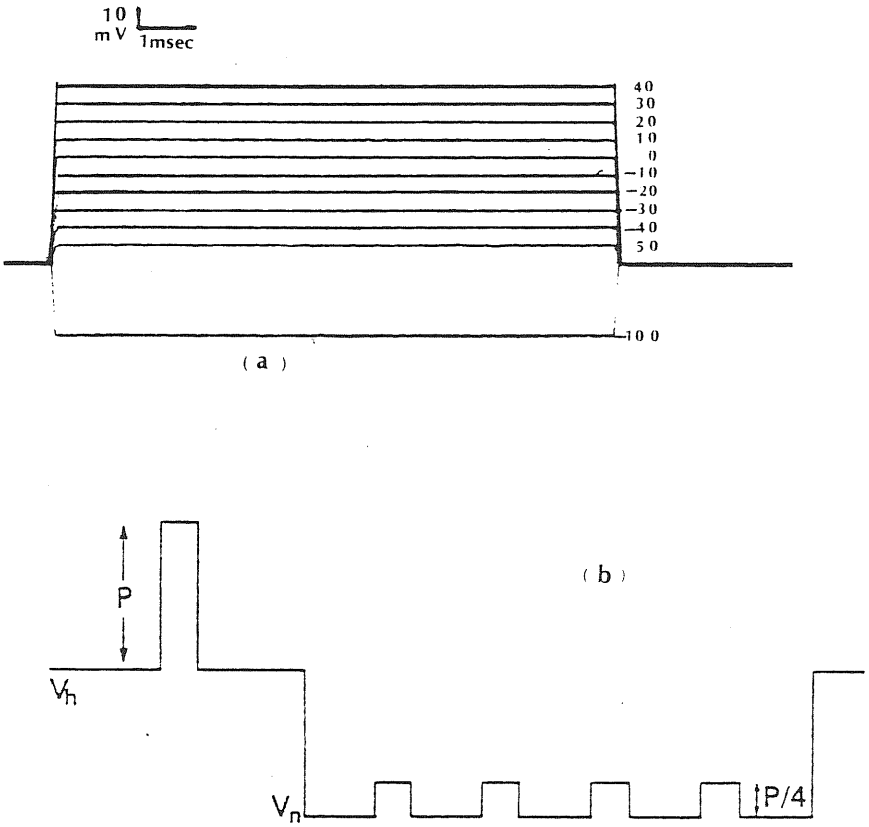

Figure 2.4:

Voltage pulse protocols.

Two kinds of voltage pulse protocols used in our experiments. Figure (a) shows the one-pulse protocol used in earlier experiments; figure (b) shows the pulse sequence for a full cycle of $P/4$ procedure. V_h is the holding potential for the test pulse $P(-60mV$ in our experiments). V_n is the holding potential of subtracting pulse ($-95mV$ in our experiment). The subtracting pulse is in the same pattern but of one-fourth the amplitude as that of test pulse [22].

subtraction of the current at pulse potential $V = -100mV$ (potential at which there is no ionic current) from the total currents. In the later improved experiments, the linear components were directly subtracted on line by the $P/4$ procedure [22].

The second set was a two-pulse experiment. It was used to measure the inactivation parameter h_∞. There were two pulses applied to the cell during the experiment, called "*conditional pulse*" and "*test pulse*". The conditional pulse varied from $-100mV$ to $-30mV$ with a duration of $39msec.$ to ensure the complete inactivation of the sodium channel. The test pulse was fixed at $-10mV$ with $4msec.$ duration. The ratio of the current with conditional pulse applied (I_{Na}) to that without conditional pulse (I_{max}) reflects the fraction of channels not inactivated, h_∞, precisely

$$h_\infty = \frac{I_{Na}}{I_{max}} \tag{2.1}$$

All the experiments were performed with a fixed holding potential of $-60mV$.

Chapter 3

Results

3.1 The action potential and whole cell sodium current

Action potential has been recorded when using the current stimulus (see figure 3.1). The sharp rise of the action potential after the inflection point indicates the sudden onset of the sodium channel, which corresponds to the flux of the inward sodium ions. The peak of the potential is approximately equal to the equilibrium potential of the sodium channel, while the droping of the potential is caused by the outward flux of the potassium ions and by the inactivation of sodium currents. The observed action potentials in granule cells have the same character as those observed in the other kinds of excitable cells [10,23].

During our experiments, we have used two methods to obtain the pure sodium currents. In the earlier experiments, TTX was added to the external solution to eliminate the sodium components in the total response currents, which separated the two components (Na and K) of the total currents. In the later experiments, CsF is added to the intracellular solution to block the potassium channel directly. The experimental results show the clear superiority of the later method in studying the sodium channel. In this chapter, we show only the results obtained in the later experiments. In chapter 4.1 we give a comparison between the

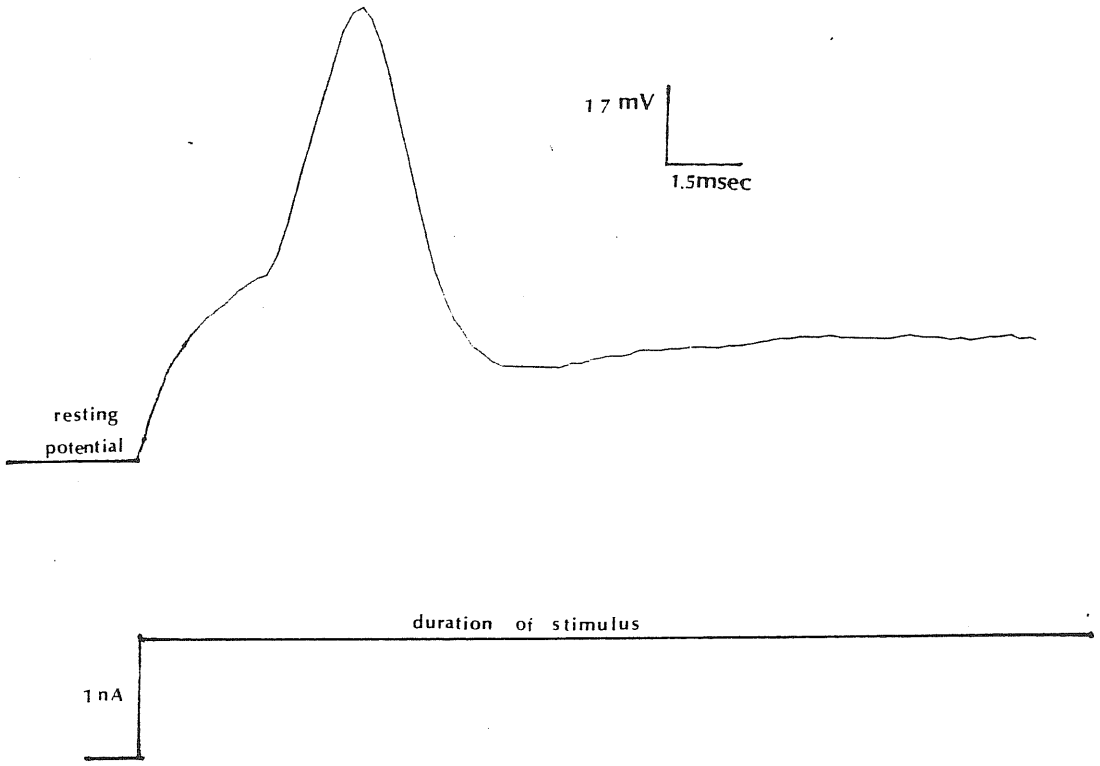

Figure 3.1:
The action potential recorded in granule cell under the current stimulus.

earlier and later experimental results.

In figure 3.2, we show a family of the whole cell sodium currents obtained in response to one-pulse depolarizations. The linear capacity and leakage components have been subtracted. The sodium current first appears at $-30mV$, and reaches its maximum value at about $-20mV$.

The $I-V$ relation (relation between the sodium current peaks I_p and the stimulating potentials V_m) of the sodium component can be obtained, by fitting the peak of each sodium current at a different potential to a third degree polynomial. Since most of sodium channels are activated at higher potentials, i.e around the reversal potential, the slope of the linear part of the $I-V$ curve at this potential may be used as maximum conductance ($\bar{g}_{Na}$). Our fitting results are plotted in figure 3.3.

3.2 Activation process of sodium channel

3.2.1 Steady state activation probability

The value of m_∞ varies with potential, it can be approximately calculated by the equation:

$$m_\infty{}^3 = \frac{g_{Na}}{\bar{g}_{Na}} \tag{3.1}$$

$\bar{g}_{Na}$ is the maximum conductance of sodium channels obtained in the $I-V$ fit. The g_{Na} is the conductance at different membrane potential V_m, calculated by Ohm's law:

$$g_{Na} = \frac{I_{peak}}{V_m - V_{rev}} \tag{3.2}$$

with V_{rev} the equilibrium potential. Values obtained in this way are plotted in figure 3.4 and can be accurately fit into the equation

$$m_\infty = \frac{1}{1+\exp(\frac{V_{1/2}-V_m}{z_{ap}})} \tag{3.3}$$

in which $z_{ap} = \frac{KT}{ze}$ represents how many millivolts are needed to increase m_∞ exponentially. $V_{1/2}$ is the potential at which $m_\infty = 0.5$ and z is the valence of the gating particle of the channel.

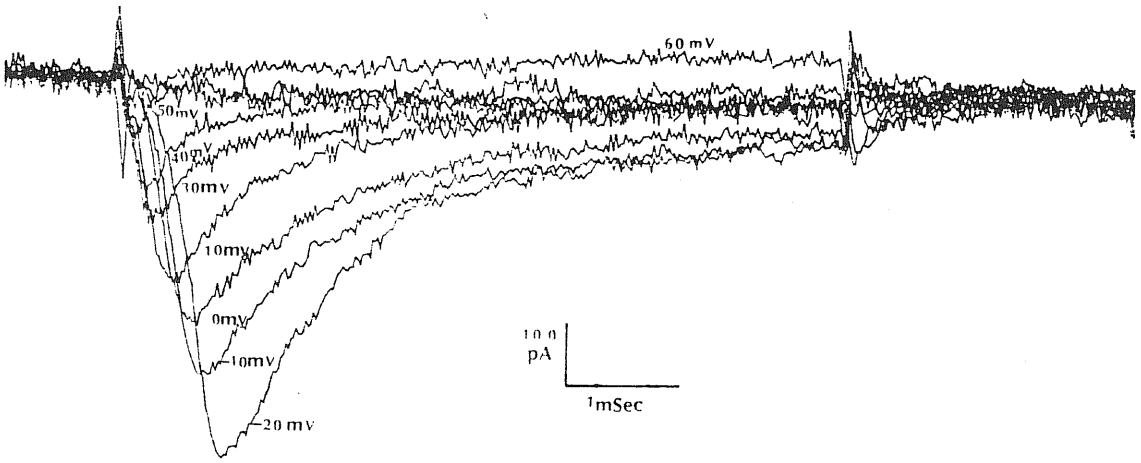

Figure 3.2:
Whole cell sodium currents recorded in cerebellar granule cell by patch-clamp technique.

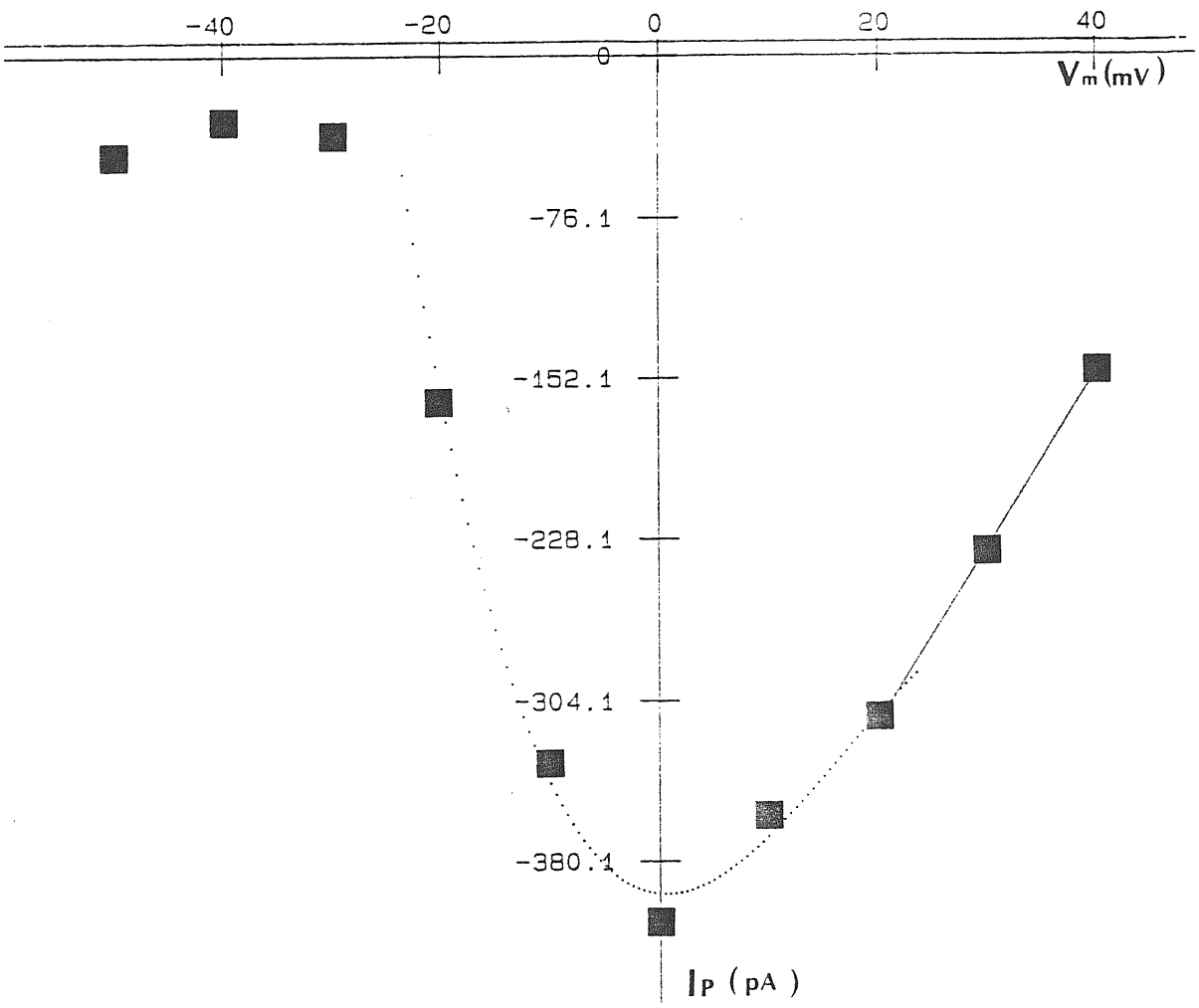

Figure 3.3:

$I - V$ relation of sodium currents.

The squares are the experimental results, the dotted line was obtained by fitting the experimental data to a third degree polynomial, which gives the maximum sodium current of $396pA$ at potential $0mV$. The maximum of conductance and the reversal potential, were evaluated by a linear fitting (solid line), and are $8158pS$ and $59mV$ respectively.

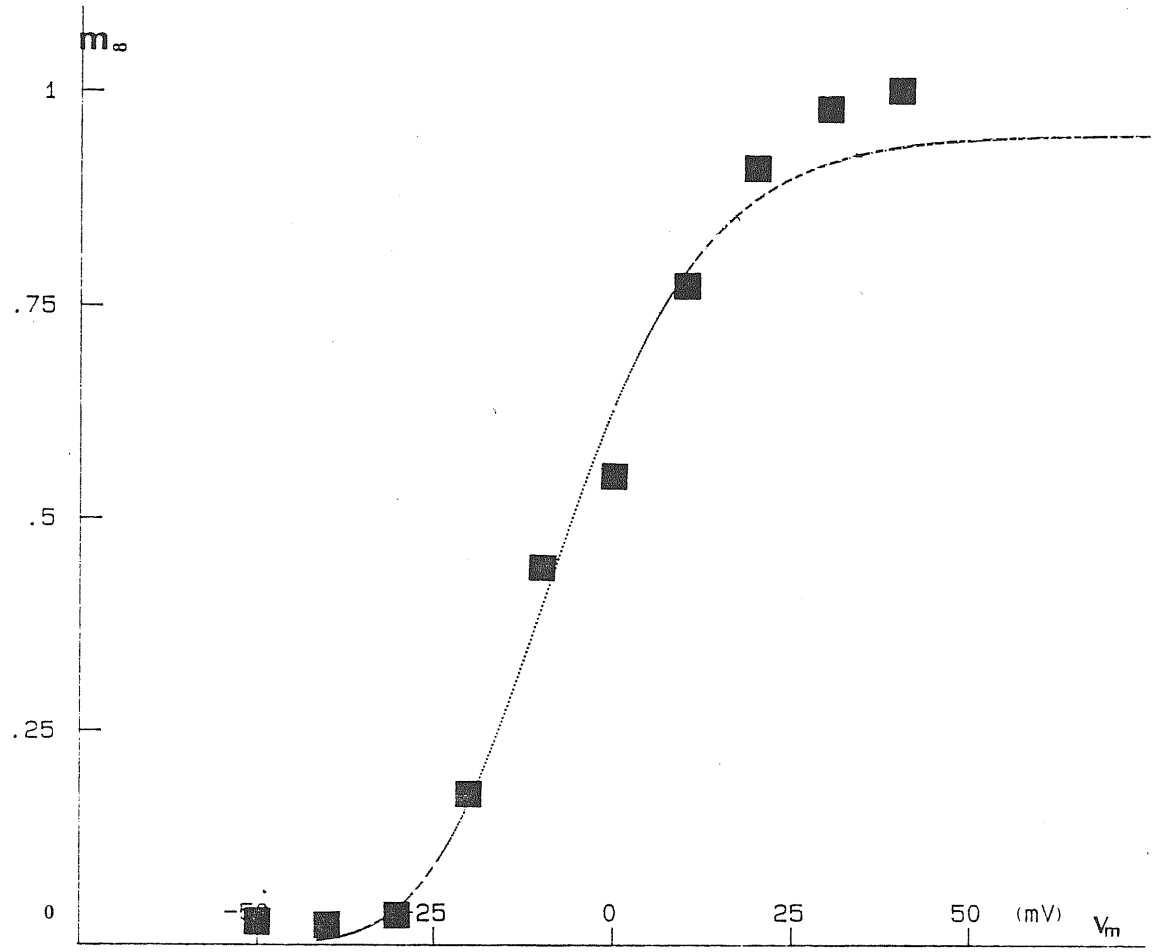

Figure 3.4:

Steady state activation probability m_∞ as a function of membrane potential.

The dotted line is obtained by fitting the experimental results (squares) with the expression 3.3. The fitting result shows that a charge $6.3e$ is involved in the activation of the Na channel.

From figure 3.4, we can see that the activation probability of the channels increases rapidly when the potential is larger than $-25mV$, and approaches asymptotically to the maximum value 1 when the potential is larger than $+25mV$. From our fitting of m_∞, it is shown that $V_{1/2} = -22mV$. Furthermore, we obtained that the charge of gating particle of the channel is $2.1e$ (where e is the electron charge unit), which means that there is $6.3e$ of charge transferred to activate the sodium channel. This value approximates to the value $6e$ predicted by the HH model [7], and is also comparable to the result obtained from gating current analysis $(6.3 \pm 0.3e)$ [24].

3.2.2 Time constant of activation process

In HH model, the kinetic parameters are described by the equation:

$$I = I'(1 - \exp(-\frac{t}{\tau_m}))^3 exp(-\frac{t}{\tau_h}) \tag{3.4}$$

where $I' = \bar{g}_{Na} {m_\infty}^3 h_o$. Fitting the Na currents with this equation will provide the values of τ_m or τ_h, as used by Hodgkin and Huxley [7,16]. However, this method is too complicated and time consuming, we instead analyzed the currents by parts. Since the inactivation is a slower process, it usually appears to be effective only after the sodium current peak. Thus we evaluate the τ_m by fitting the onset parts of sodium currents, which are composed almost entirly from activation components, to equation 3.5:

$$I = I'(1 - \exp(-\frac{t}{\tau_m}))^3 \tag{3.5}$$

The activation time constants τ_m in our experiments were measured only at voltages larger than $-50mV$, due to the limited sensitivity of the measurement of the current. The potential dependence of the time constant of the activation process obtained in our experiment is shown in figure 3.5. It shows that the process of activation becomes faster (smaller τ_m) with the increase of membrane potential.

We have recorded the sodium currents at different temperatures. From our experimental results, it seems that there are obvious changes

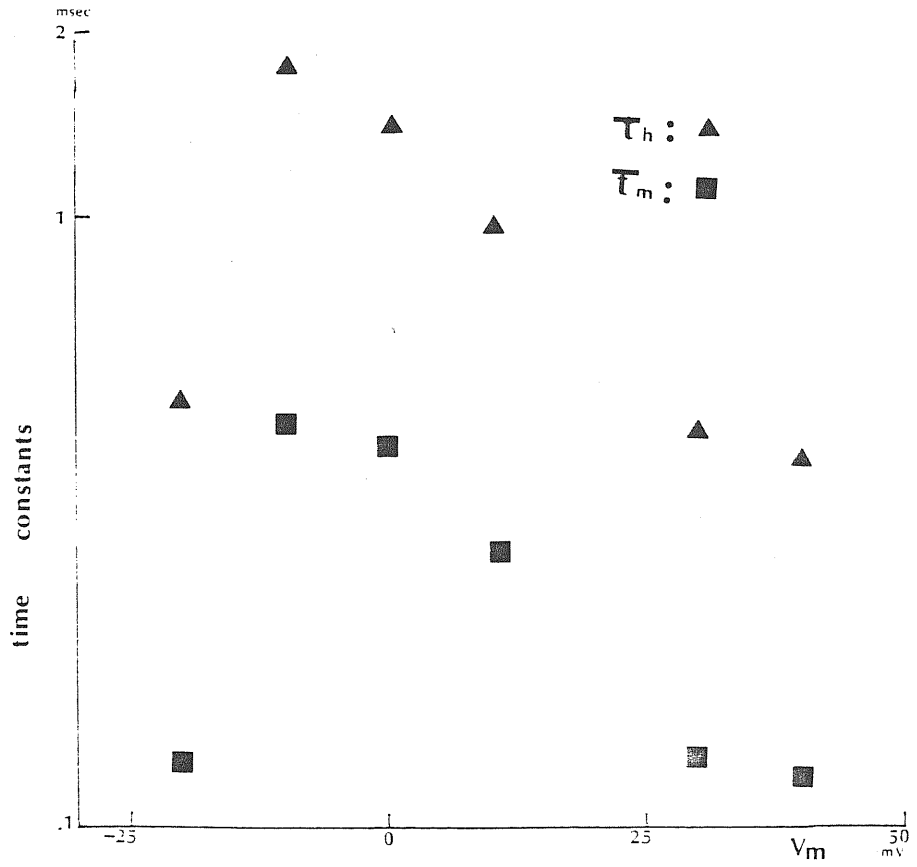

Figure 3.5:

The dependence of the time constants on membrane potential V_m

The time course of the inactivation (triangles) process of sodium current is slower with respect to the activation process (squares).

in the values of the activation time constants at different temperatures. Figure 3.6 shows the τ_m measured at two temperatures, $28°C$ and $20°C$. It is found that the activation process is faster at higher temperature.

3.3 Inactivation process of sodium channel

3.3.1 Steady state inactivation probability

Experimentally, we varied the conditional potentials to obtain the voltage dependence of the inactivation probability h_∞. We have obtained h_∞ values by directly using the equation 2.1. The results obtained are then fit to the equation:

$$h_\infty = \frac{1}{1 + \exp(\frac{V_{cp} - V_{1/2}}{z_a p})} \tag{3.6}$$

where V_{cp} is the conditional pulse potential, $V_{1/2}$ is the potential at which $h_\infty = 0.5$, and $z_{ap} = \frac{KT}{ze}$ represents the potential in millivolts needed to increase h_∞ exponentially.

It indicates that as the conditional potential is larger than $-80mV$, the peak values of sodium currents begin to decrease, and the channels appear to be completely inactivated for conditional potentials larger than $-25mV$. We give the experimental results for h_∞ in figure 3.7. The fitting results show that the probability of the channel inactivation reaches 0.5 when the applied conditional potential equals to $-34.4mV$. We obtained the value $4.3e$ of the charge transferred to inactivate the channel. The quantity of charge transferred for inactivation is therefore smaller than that needed for activation.

3.3.2 Time constant of inactivation process

In our experiments, the inactivation time constants τ_h were measured only at voltages larger than $-50mV$ (due to the same reasoning as for

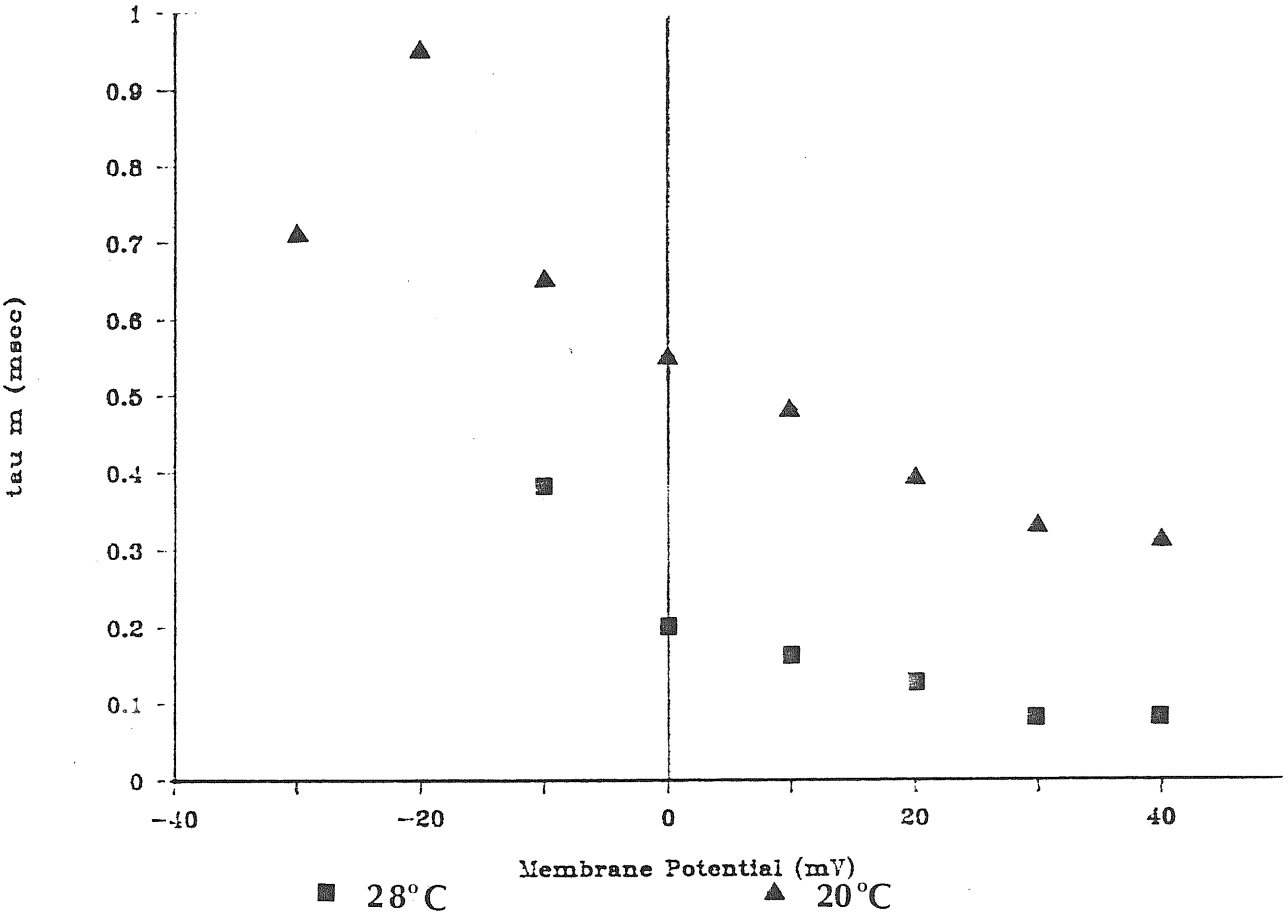

Figure 3.6:

Temperature dependence of τ_m.

It is found that the temperature may influence the activation process. The higher the temperature, the faster the activation process is.

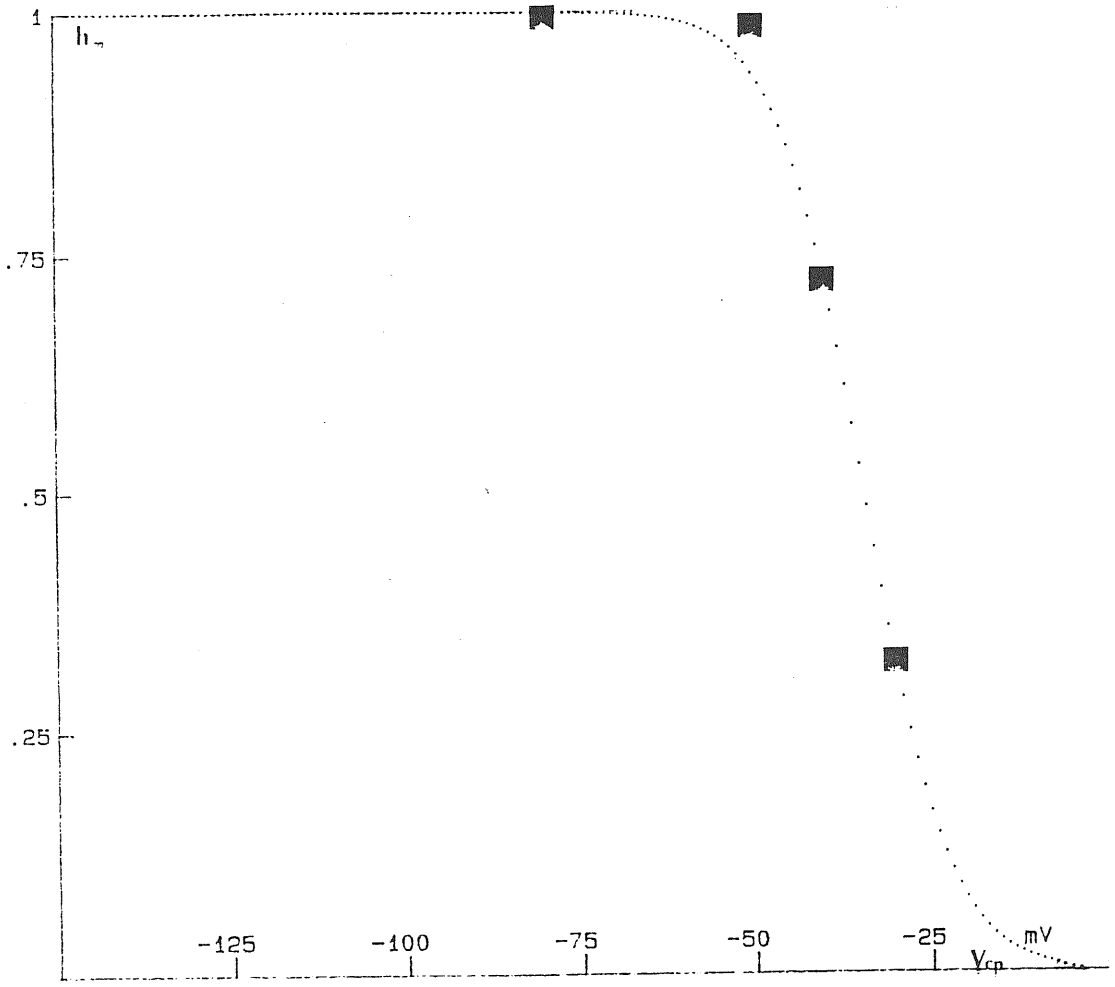

Figure 3.7:

Potential dependence of the inactivation probability h_∞.

The data points in the figure are the experimental values according to equation 2.1. The dotted line is obtained by fitting the experimental results to equation 3.6.

τ_m), but were obtained by fitting the offset parts of the sodium currents (see figure 3.2) by equation

$$I = I' \; exp \; (-\frac{t}{\tau_h}) \tag{3.7}$$

Plotting the experimental data in figure 3.5, we clearly see that the inactivation process is also faster at higher potentials, however, it is still slower than the activation process, which is what the HH model predicted (see chapter 1, compare also the figure to the figure 1.6).

Chapter 4

Discussion

4.1 Discussion

Using the usual cell separation procedure, we have carried out two kinds of experiments on the dissociated rat cerebellar granule cells in primary culture:

- Recording of the action potentials with external current stimuli;
- The whole cell patch clamp sodium current recording.

Our experimental results show that granule cells from rat cerebellum have TTX-sensitive sodium channels. The sodium channels can be completely blocked by TTX. Potassium and sodium currents are the main components of the response currents, but Ca seems not to contribute. We have found that the permeability changes of the sodium channels in rat granule cells can be described by the HH model. Two processes exist: The activation process and inactivation process, the former faster. We have also verified that the activation time constant τ_m is temperature dependent.

4.1.1 Properties of sodium channel in rat granule cell

It is possible to estimate the membrane area of the patched cell from the membrane capacity obtained after membrane capacity compensation, using the empirical relation: $1pF$ of membrane capacity corresponds to $0.01\mu m^2$ of membrane area. The current density of the cell can be obtained as the ratio of peak value of the sodium current to the area of the cell membrane. As shown in table 4.1, the peak Na current density in the rat granule cell is comparable to those in other neurons such as chick dorsal root ganglion (DRG) [4] and rat pituitary GH3 [5]. Assuming elementary current amplitude $i = 0.7pA$ with open probability of the channel at maximum activation $P = 0.5$ [25], we found that Na channel density in our granule cell is $4.83/\mu m^2$. Under the same assumptions, we find that this density is also comparable to those in chick DRG [4] and rat pituitary GH3 [5]($5.68/\mu m^2$). Table 4.2 lists the values of activation time constants τ_m obtained in different excitable cells. The activation processes are found to be comparable to each other.

As described in chapter 3, we showed the temperature dependent property of τ_m. We have also compared the values of τ_h at $T = 20°C$ and those at $T = 28°C$. It seems that τ_h is less temperature dependent. However, this should be retained with caution because most of the results at $T = 20°C$ were obtained by the earlier method. These currents usually contain substantial K current residues and this may alter the measurement of τ_h. Further experiments at $20°C$ with the later method are necessary to prove this point. Table 4.3 shows the τ_h values measured in different cultured cells. The τ_h in the granule cell is comparable to those in most of the other excitable cells [7,6,4,30].

4.1.2 Comparision of the earlier and later experiments

As we have described in section 2.5, the sodium currents were obtained in the earlier experiments, by using TTX as blocker, which was

Cells	$I_p[mA/cm^2]$	$V_m[mV]$	$Temp.[\,^\circ C]$
Squid axon [7]	1.30	-10	5
Frog node [26]	13	-20	20
Snail neuron [27]	0.5	-6	13.5
Mouse neuroblastoma [28]	0.4	-10	20
Bovine chromaffine [29]	0.06	10	20
Rat pituitary GH3 [30]	0.1	12	22
Rat pituitary GH3 [5]	0.2	0	22
Rat dorsal root ganglion neuron (DRG) [31]	0.07	-25	20
Guinea pig DRG [32]	2.5	0.	20
Chick DRG [33]	0.5	10	25
Chick DRG [4]	0.2	-10	12
rat granule cell (*)	0.17	0	28

Table 4.1:

The peak sodium current density (I_p) in excitable cells.

Here, V_m is the membrane potential at which the I_p is measured. Temp. is the experimental temperature. The data with (*) is the present result.

Cells	$\tau_m[ms]$	$V_m[mV]$	$Temp.[\,^\circ C]$
Squid axon [7]	0.51	-40	6
Rat brain Na channel [37]	0.40	-40	20
Rat granule cell (*)	0.44	-10	28

Table 4.2:

The parameter τ_m in various excitable cells.

Here, V_m is the membrane potential at which τ_m is measured. Temp. is the experimental temperature. The data with (*) is the present results.

Cells	$\tau_h[ms]$	$V_m[mV]$	$Temp.[\ ^\circ C]$
Squid axon [7]	1.50	0	6
Myxicola axon [6]	1.50	-3	5
Crayfish axon [34]	0.45	0	8
Aplysia neuron [27]	18	-6	13.5
Frog node [35]	0.5	0	20
Rabbit node [36]	0.9	-35	14
Mouse neuroblastoma [28]	0.5	-8	20
Chick dorsal root ganglion neuron [4]	1.5	0	12
Bovine chromaffine [29]	1.2	0	20
Rat pituitary GH3 [30]	2.2	0	20
Rat pituitary GH3 [5]	1.1	20	20
Rat granule cell (*)	1.75	-10	28

Table 4.3:

The parameter τ_h in various excitable cells.

Here, V_m is the membrane potential at which τ_h is measured. The Temp. is the experimental temperature. The data with (*) is the present results.

an indirect method. This approach consisted of two steps: i) obtaining the controlled total currents, as well as the potassium currents by adding TTX in the external solution; ii) subtracting the potassium currents from the total currents. Two sets of current recordings were thus needed under the *same set of potentials*, thus the earlier experiments were time consuming. Furthermore, the patch condition always changed during such a long recording due to the mobility of the broken membrane lamellas under the pipette. Therefore, the broken hole of the patched membrane was often reduced and caused substantial increase of the series resistance (see section 4.1.3). The increase of resistance not only determines a drop of the potential across the membrane, but also causes a longer delay of the ionic current onset (remember that the onset time $\tau = RC_{membrane}$). Because of the previously discussed reasons, the stimulating pulses are not always identical in the two sets of recordings. This produces artifacts, due to the substantial residues of the potassium and capacity components, as suggested by figure 4.1.

We have improved the experiments by using CsF blocker (later experiments). The Cs ions can enter the K channels from the intracellular solution and block the outward flow of the potassium ions. As this new method directly measures the sodium current, it is much less time consuming, so the patch condition is more stable, avoiding the difficulties encountered in the earlier experiments. In most of our later experiments, the K component eliminations are complete (see figure 3.2).

Notwithstanding there are defects of the earlier experiments mentioned above, there is no difference between the properties of sodium currents (m_∞, τ_m, h_∞, τ_h) obtained by the two approaches.

4.1.3 Series resistance compensation

Series resistances are introduced in the electrical pathway between the output of patch amplifier and the patched cell. The presence of the series resistance will cause the drop of a voltage across the membrane, which gives rise to an underestimated membrane potential. The series resistance is usually very large, ranging from $5M\Omega$ to $20M\Omega$, so that the

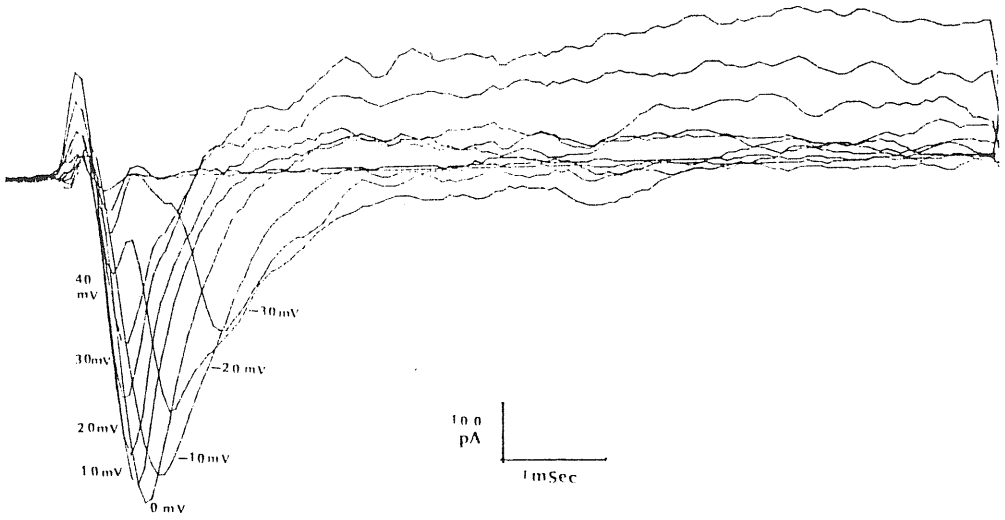

Figure 4.1:

A sodium current family obtained in the earlier experiments.

Due to changes of the patch condition, the potassium components still remain.

$G_{series}[mS]$	Potential drop σ [mV]
0.02	42
0.045	22
0.049	8.49
0.136	4.7

Table 4.4:
Estimation of the error σ for the potential under different compensation of series resistance $\frac{1}{G_{series}}$. The conductances G_{series} are in unit millisiemens (mS).

voltage errors can be considerably larger when the cell currents are large, which occurs quite often for whole cell current recordings. Empirically, we find that the series resistance effect is quite important when the cell current is larger than $1nA$. Furthermore, the large value of series resistance also causes large time delay of ionic current, since more time is needed to charge the membrane capacitance (see section 4.1.2).

In compensating the series resistance, the membrane voltage estimation error caused by the series resistance can be estimated electronically. In table 4.4, we present the membrane voltage estimation errors after different series resistance compensations.

Ideal compensation should keep the voltage drop smaller than $2mV$; however, from our experience this is very difficult, because the compensating circuit tends to excite oscillation of the current, which could damage the very fragile granule cells.

4.2 Conclusions

We have undertaken a series of experimental studies of the permeability changes of sodium channels with external electric stimuli. The results demonstrated that the model proposed by Hodgkin and Huxley is also applicable to the excitable granule cell of rat cerebellum. From our experiments, it is shown that the channel density in the granule cell

is comparable to those measured in other neurons (see table 4.1), as the time constants of activation and inactivation processes (see table 4.3 and table 4.2). The temperature dependence of the parameter τ_m is obtained. However, more specific experiments are needed to study the temperature dependence of τ_h.

Due to the fragile character of the granule cell, the series resistance compensation is still to be optimized. The optimization requires a systematic improvement over the traditional compensation method.

Bibliography

[1] B. Hille, Ionic channels of excitable membranes, Sinauer associates inc., Sunderland, Massachusetts (1984)

[2] O. P. Hamill, A. Marty, B. Sakmann and F. J. Sigworth, Improved patch-clamp techniques for high-resolution current recording from cells and cell-free membrane patches. *Pflügers Arch.* **391**, 85 (1981)

[3] A. Borsellino, Z. Galdzicki, A. Novelli, G. Puia, M. Sciancalepore, Developmental changes in the electrophysiology of cerebellar granule cells in primary culture. Poster in 11th Annual Meeting of The European Neuroscience Association. (Zürich, Switzerland), (1988)

[4] E. Carbone, H. D. Lux, Sodium Channels in cultured chick dorsal root ganglion neurons. *J. Eur. Biophys.***13**, 259 (1986)

[5] D. R. Matteson, C. M. Armstrong, Na and Ca channels in a transformed line of anterior pituitary cells. *J. Gen. Physiol.* **83**, 371 (1984)

[6] L. Goldman, C. L. Schauf, Quantitative description of sodium and potassium currents and computed action potential in *Myxicola* giant axons. *J. Gen. Physiol.* **61**, 361 (1973)

[7] A. L. Hodgkin and A. F. Huxley, A quantitative description of membrane current and its application to conduction and excitation in nerve. *J. Physiol. (Lond.)* **117**, 500 (1952)

[8] K. S. Cole, Membranes, ions and impulses: A Chapter of Classical Biophysics, Univ. of Cal. Press, Berkeley, 569 (1968)

[9] W. Nernst, Zur Kinetik der Lösung defindlichen Körper: *Theorie der Diffusion. Z. Phys. chem.*, 613 (1888)

[10] K. S. Cole and H. J. Curtis, Electric impedance of Nitella during activity, *J. Gen. Physiol.* **22**, 649 (1939)

[11] A. l. Hodgkin and B. Katz, The effect of sodium ions on the electrical activity of the giant axon of the squid. *J. Physiol. (Lond.)* **108**, 37 (1949)

[12] G. Marmont, studies on the axon membrane. I. A new method. *J. Cell Comp. Physiol.* **34**, 351 (1949)

[13] K. S. Cole, Dynamic electrical characteristics of the squid axon membrane, *Arch. sci. physiol.* **3**, 253 (1949)

[14] A. L. Hodgkin, A. F. Huxley and B. Katz, ionic currents underlying activity in giant axon of the squid. *Arch. Sci. Physiol.* **3**, 129 (1949)

[15] A. L. Hodgkin, A. F. Huxley and B. Katz, Measurements of current-voltage relations in the membrane of giant axon of *Loglio. J. Physiol. (Lond.)* **116**, 424 (1952)

[16] A. L. Hodgkin and A. F. Huxley, The dual effect of membrane potential on sodium conductance in the giant axon of *Loligo. J. Physiol. (Lond.)* **116**, 497 (1952)

[17] A. L. Hodgkin and A. F. Huxley, Currents carried by sodium and potassium ions through the membrane of the giant axon of *Loligo. J. Physiol. (Lond.)* **116**, 449 (1952)

[18] A. L. Hodgkin and A. F. Huxley, The components of membrane conductance in the giant axon of *Loligo. J. Physiol.* **116**, 473 (1952)

[19] A. L. Hodgkin, Ionic movements and electrical activity in giant nerve fibres. *Proc. Royal Soc. Lond. B.* **148**, 1 (1958)

[20] B. Hille, Ionic channels in nerve membranes., *Prog. Biophys. Mol. Biol.* **21**, 1 (1970)

[21] O. R. Sayan, Primary Neuron Culture: Isolation of Glutamatergic Cerebellar Granule cell from eight day old Sprague Dawley rat. *Internal report from National Institutes of Health* (1987)

[22] F. Bezanilla and C. M. Armstrong, Inactivation of the sodium channel, I. Sodium current experiments, *J. Gen. Physiol.* **70**, 549 (1977)

[23] H. Meves, Thirty years after. *Current topics in membranes and transport*, **22**, 279 (1984)

[24] M. F. Schneider and W. K. Chandler, Voltage-dependent charge movement in skeletal muscle: *A possible step in excitation-contraction coupling. Nature (London)* 242, 244 (1973)

[25] F. J. Sigworth, The variance of sodium current fluctuations at the node of Ranvier. *J. Physiol.* **307**, 97 (1980)

[26] F. A. Dodge, B. Frankenhäuser, Sodium currents in the myelinated nerve fibre of *Xenopus Laevis* investigated with the voltage clamp technique. *J. Physiol. (Lond.)* **148**, 188 (1959)

[27] D. J. Adams, P. W. Gage, Characteristics of sodium and calcium conductance changes produced by membrane depolarization in an *Aplysia* neurone. *J. Physiol. (Lond.)* **289**, 143 (1979)

[28] W. H. Moolenar, I. Spector, Ionic currents in cultured mouse neuroblastoma cells under voltage-clamp conditions. *J. Physiol. (Lond.)* **278**, 265 (1978)

[29] E. M. Fenwick, A. Marty, E. Neher, Sodium and calcium channels in bovine chromaffin cells. *J. Physiol. (Lond.)* **331**, 599 (1982)

[30] J. M. Dubinsky, G. S. Oxford, Ionic currents in two strains of rat anterior pituitary tumor cells. *J. Gen. Physiol.* **83**, 309 (1984)

[31] P. G. Kostyuk, N. S. Veselovsky, S. A. Fedulova, Ionic currents in the somatic membrane of rat dorsal root ganglion neurons. *Neuroscience* **6**, 2431 (1981)

[32] M. Kameyama, Ionic currents in cultured dorsal root ganglion cells from adult guinea pigs. *J. Membr. Biol.***72**, 195 (1983)

[33] K. Dunlap,G. D. Fischbach, Neurotransmitters decrease the calcium conductance activated by depolarization of embryonic chick sensory neurons. *J. Physiol. (Lond.)* **317**, 519 (1981)

[34] R. P. Swenson, Gating charge immobilization and sodium current inactivation in inactivation in internally perfused cryfish giant axons. *Nature (Lond.)* **287**, 644 (1980)

[35] B. Frankenhäuser, Inactivation of the sodium-carrying mechanism in myelinated nerve fibres of *Xenopus Laevis*. *J. Physiol. (Lond.)* **169**, 445 (1968)

[36] S. Y. Chiu, J. M. Ritchie, R. B. Rogart, D. Stagg, A quantitative description of membrane currents in rabbit myelinated nerve. *J. Physiol. (Lond.)* **292**, 149 (1979)

[37] W. Stühmer, C. Methfessel, B. Sakmann, M. Noda, S. Numa, **Patch clamp characterization of sodium channels expressed from rat brain cDNA.** *Eur. Biophys. J.* **14** 131 (1987)

Acknowledgements

I wish to express my gratitude to the continuous support of professor Antonio Borsellino. I am grateful to the collaboration of Dr. Zygmunt Galdzicki from **Department of Biophysics, Academy of Medicine, Poland** and Drs. Giulia Puia and Marina Sciancalepore from the **Biophysics Laboratory**, here, in **International School for Advanced Studies** in Trieste, Italy. They have given important contributions in the cell preparations and experimental recordings. I have had very helpful discussions with Dr. Oscar Moran, also from the **Biophysics Laboratory**, during the data analysis and the present handwriting, to him I want to express my gratitude. I would like to express my gratitude to Dr. Antonello Novelli, from **National Insititutes of Health, USA**, for his helpful suggestion about the cell culture, and to Mrs. Judy Geiger for her warm helps in English.